Ivan Fomin*, Robert Odenbach, Enrico Pannicke, Bennet Hensen, Frank Wacker, Georg Rose

µRIGS – Ultra-light Micropositioning Robotics for Universal MRI Guided Interventions

Abstract: Performing minimal invasive interventions under real-time image guidance proves problematic in a closed-bore magnetic resonance imaging scanner. To enable better usability in MRI guided interventions, robotic systems could be used for additional assistance. However, the integration of such devices into the clinical workflow relates to many technical challenges in order to increase precision of the procedure while ensuring the overall safety.

In this work, an MR compatible, compact, ultra-light and remotely controllable micropositioning system called µRIGS is presented. The instrument positioning unit can be operated in a 5-DoF range within a working volume of 2100 cm^3 with an instrument feed of 120 mm. The kinematics are actuated with a combination of non-metallic Bowden cables and electric stepper motors from a safe distance inside the scanner room, while their control is initiated from the control room via a custom-fitted GUI.

Thereby, the precision of the positioning reproducibility of the respective DoF can be achieved with a mean deviation of 0.12°. Furthermore, a feed force of 14 N can be provided to puncture various soft tissue.

Keywords: MR compatible, Ultra-light, Patient-mounted, Robot, Manipulator, Positioning system, Image-guided surgery, MRI guided Intervention

https://doi.org/10.1515/cdbme-2021-1018

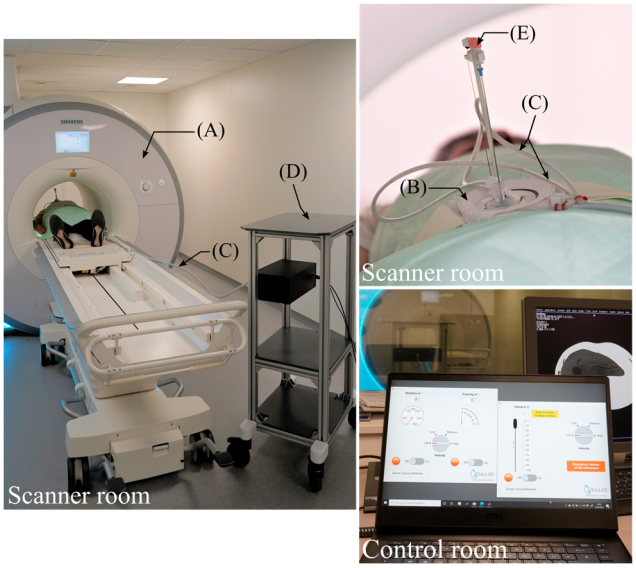

Figure 1: µRIGS exemplary in the clinical setup for performing an MRI guided liver puncture with an 3 T Skyra System (A). The Instrument positioning unit (B) with 5-DoFs can be remotely controlled from the control room via Bowden cables (C) and the drive unit installed on a mobile and MR safe trolley (D). (E) 18 G puncture needle.

1 Introduction

Compared to sonography (US) or computed tomography (CT), magnetic resonance imaging (MRI) offers high soft tissue contrast as well as real-time multiplanar imaging capabilities for navigation. In addition, MRI has the unique ability to measure temperature distribution non-invasively. These aspects form the basis for performing MRI guided diagnostic procedures (e.g. biopsy) and minimally invasive therapeutic interventions (e.g. tumor ablation, pain therapy and brachytherapy). [1–3]

Despite many advantages, some disadvantages complicate the application in clinical practice, such as the constricted space in the MR bore or the non-standardized workflows, which currently limit interventional MRI (iMRI) to relatively small number of cases in specialized centers [1]. In particular, positioning and continuously holding the

***Corresponding author: Ivan Fomin,** Research Campus *STIMULATE*, Otto-von-Guericke University, Magdeburg, Germany, E-Mail: ivan.fomin@ovgu.de

Ivan Fomin, Robert Odenbach, Enrico Pannicke and Georg Rose, Institute for Medical Engineering, Otto-von-Guericke University, Magdeburg, Germany

Bennet Hensen and Frank Wacker, Institute of Diagnostic and Interventional Radiology, Medical School, Hannover, Germany

Enrico Pannicke, Bennet Hensen, Frank Wacker and Georg Rose, Research Campus *STIMULATE*, Otto-von-Guericke University, Magdeburg, Germany

instrument while manually navigating through image-based planes of an anatomical region to the target proves highly challenging. Furthermore, MR-compatible tools face many challenges in development, making it difficult to use a variety of cost-effective technologies [4].

To increase efficiency and effectiveness in iMRI, the state of the art includes various positioning manipulators and MRI robots for guiding instruments [5–6]. However, only a few systems have been established in clinical use so far due to bulky dimensions for limited regions of application as well as complex installation and operation procedures [7–8]. For clinical practice high precision systems that are easy, fast and versatile to set up are needed to reduce the complication rate in iMRI effectively.

To counteract the present difficulties, an intuitive, MR-compatible, compact and remotely controllable micropositioning robot called µRIGS to assist automated interventions on different anatomical application areas (trunk and extremities) will be presented as a first demonstrator in this work and analyzed in its general performance.

2 Materials and methods

On the hardware side, µRIGS is basically composed of the instrument positioning unit (IPU) and the drive unit (DU), which initiates the motion sequences at the IPU remotely. All hardware is placed inside the scanner room and controlled from the control room using a host computer with an associated graphical user interface (GUI) (see Figure 1). The individual components are presented in the following chapter.

2.1 Instrument positioning unit

The IPU serves as a core element of the µRIGS to precisely position different instruments (e.g. coaxial needle) within the MRI bore using appropriate kinematics. In this context, the selection of MR safe materials is of particular interest. The demonstrator is mainly made of 3D printed polyethylene terephthalate plastics and glass fiber reinforced polymer. Sliding sleeves, sliding foils as well as MR compatible ball bearings from igus® (Cologne, Germany) serve as standard components for low-friction motion sequences of the mechanical parts. Figure 2 shows the basic mechanical components and their kinematic functions within the IPU. In total, five degrees of freedom (DoF) are provided via two rotational axes and three translational axes. The main positioning is done via three DoF in a spherical coordinate system. This includes the central unit (Fig. 2; 1-2), which

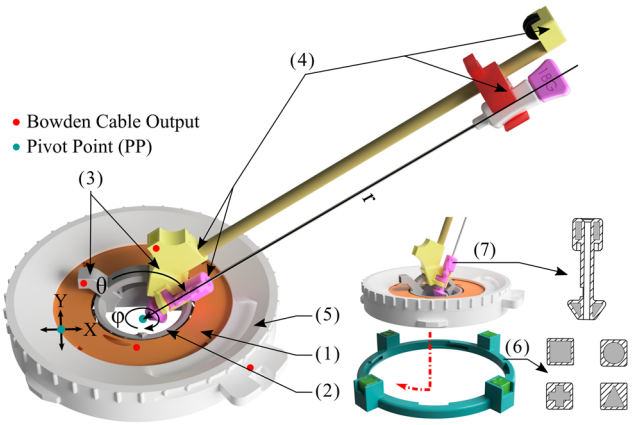

Figure 2: Mechanical and kinematic elements of the IPU. (1-2) Central unit. (3) Arc portal unit. (4) Instrument feed unit. (5) Base unit. (6) MR visible bayonet adapter ring. (7) Instrument guide sleeve as MR visible marker. (rotation) $\varphi = 0 - 360°$. (panning) $\theta = 0 - 55°$. (feeding) $r = 0 - 120\,\text{mm}$. (lateral movement of the PP) $XY = 20\text{x}20\,\text{mm}$.

provides the adjustment of the azimuth angle φ (rotatin). The arc portal unit (Fig. 2; 3) provides a panning motion to adjust the polar angle θ. Furthermore, the instrument feed unit (Fig. 2; 4) serves as kinematic sequence to adjust the feed length r through the pivot point (PP), which represents the insertion point on the skin surface simultaneously. The base unit (Fig. 2; 5) provides the alignment of the central unit in the Cartesian XY plane as the 4th and 5th DoF if correction of the insertion point becomes necessary without repositioning the IPU on the skin. The kinematic behavior of the main DoF always remain unchanged if the PP is moved within the XY plane. The IPU dimensions are adapted to a coaxial 18 G puncture needle (Innovative Tomography Products GmbH, Bochum, Germany) with an active length of 150 mm. The overall size of the IPU is about 115 mm in diameter and a maximum height of 175 mm. Besides, the geometry of the instrument guidance sleeve (Fig. 2; 7) can be customized to common needle diameters.

Specific fixation devices of the IPU are intended to ensure a quick and intuitive fixation directly on the skin of the patient on different areas of application (trunk or extremities) as well as a fast removal function for safety purposes in emergency cases. The basis for this universal task is a bayonet lock, which connects the IPU to the adapter ring (Fig. 2; 6) with a manual plug-in and rotary-lock movement. In combination with the manually unlockable instrument guidance sleeve (Fig. 2; 7), the IPU can be removed while the instrument remains inside the patient without removing it.

To analyze the overall orientation of the IPU and its current trajectory in the image data set, four cuboids (10x10x14 mm) act as passive fiducial markers (Fig. 2; 6)

with differently shaped cavities. The instrument guidance sleeve contains two cylindrical cavities (Fig. 2; 7), one above the other surrounding the needle. These cavities are filled with liquid VisiJet® SL Clear resin (properties of polycarbonate) during the stereolithography procedure using the ProJet 6000 SLA printer (3D-Systems Corp., CA, USA). [9]

2.2 Drive Unit

An important component to transmit initiated motions at the IPU from a safe distance (3 m) by the DU reliably and reproducibly are Bowden cables [10]. The essential basic component is the non-metallic high performance pull cord, which has a smooth surface to minimize friction to the traction sleeve that is made of polytetrafluoroethylene over the entire length [11]. The low inherent elasticity of pull cords supports reproducible travel of the mechanical components of the IPU. In total, ten Bowden cables are required to control the 5-DoF (two pull cords per DoF with opposite effective direction), which are integrated as a strand in one single polyvinyl chloride hose to stabilize the overall performance.

To execute the kinematic motion sequences the Bowden cables end up rigidly connected on multiple cable drums to wind and unwind the pull cords via a combination of worm gears and electrically powered stepper motors for a precise control. To operate the 5-DoF remotely, seven sub modules are required (shown in Figure 3). To perform the rotational motion of the inner ring (central unit), the panning of the carriage (arc portal unit) and the feed of the instrument in both directions, one sub module is required in each case, with two pull cords attached to the respective cable drum. The four remaining modules are used for the lateral displacement of the central unit in the XY plane. Each motor is controlled by a stepper motor driver, which in turn is controlled by an adapter board from an Arduino Mega 2560.

To counteract possible radio-frequency artifacts in the MR image data (can be caused by electromechanical and electrical modules), all components of the DU are placed in a

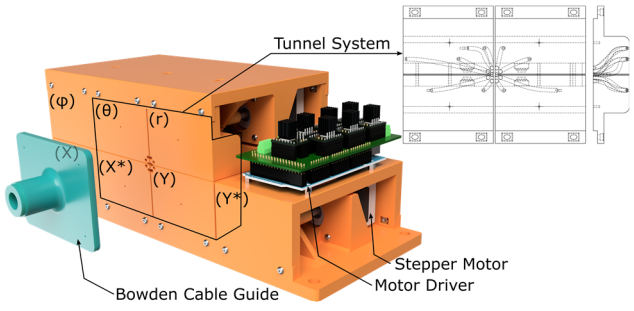

Figure 4: DU consisting of the drive submodules and the motor driver for each DoF. The tunnel system distributes each Bowden cable to its respective cable drum.

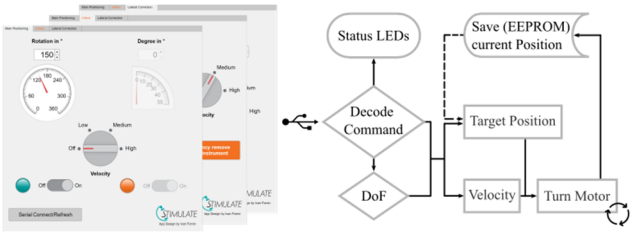

Figure 3: Control concept of µRIGS. (left) GUI as primary with all kinematic controls structured in three pages. (right) Firmware of the motor control as secondary.

shielded aluminum housing to support noise immunity and emission suppression. Peripheral connections and a user interface on the housing enable a communication interface between the DU and the host computer.

2.3 Software

The system control is built according to the primary/secondary method shown in Figure 4. The software to perform the motion sequences of all motors is embedded as a firmware on an Arduino Mega 2560 (secondary module). A GUI, based on MATLAB® (The MathWorks Inc., Version 2018b, MA, USA), serves as the primary. With this, the user specifies the status, the target position of the respective kinematic motion sequence of the IPU as well as the speed of the motors. The communication of the executed commands between primary (in the scanner room) and secondary (in the control room) proceeds via USB cable.

2.4 Kinematic analysis

A kinematic analysis of the implemented motion sequences is intended to describe the working volume that can be covered during a puncture procedure. Lateral displacement of the PP in the XY plane creates an insertion area with a quadratic base of 20x20 mm. On each adjustable PP, the 150 mm long puncture needle can reach a maximum feed length r of about 120 mm in a spherical coordinate system with $\varphi = 0 - 360°$ and $\theta = 0 - 55°$. Thus, reachability with a maximum diameter of 216 mm and a working volume of about 2100 cm^3 is possible (see Figure 5a).

2.5 Experimental setups

The evaluation of the MR visibility of the IPU is performed by acquiring test images of the printed markers on the 3T Skyra Siemens system (Siemens Healthineers, Erlangen, Germany) using a 32-channel head coil. A T1-weighted FLAIR sequence

is used to visualize the spatial arrangement of the markers as a 3D scan.

To assess the reliability of the instrument feed into different tissue types, the maximal feed force that can be applied by the IPU is analyzed. Therefore, a force gauge (SAUTER GmbH, Balingen, Germany) is mechanically connected to the head (Fig. 2, 4 – red) of the instrument feed unit to measure its tensile force until there is no more instrument feed movement measurable and the traction sleeve starts to compress significantly. The maximum measured tensile force serves as an indicator for the available feed force of the IPU.

An important system property of robotic technologies is their positioning accuracy. Since the presented µRIGS demonstrator has no direct positioning feedback installed on its moving components of the IPU, the absolute deviation shall be analyzed in the context of positioning reproducibility. A Moiré Phase Tracking (MPT) system (Metria Innovation, WI, USA) is used to study the rotational and panning motion in air determined by the φ and θ angle settings. Here, the position of an MPT marker in the Cartesian coordinate system of the MPT camera is precisely determined and converted into spherical coordinates. This marker is placed at the head-side of the clamped puncture needle at a distance of 250 mm below the MPT camera to cover the kinematic processes of the IPU within the field of view of the camera.

3 Results and discussion

3.1 MR visibility

Figure 5b shows the outer markers clearly visible in the specific shape (cross, square, circle, triangle) and intensity, which were placed in the bayonet adapter ring to ensure visibility of the entire IPU and its position in space. In the center area the two marker volumes of the instrument guidance sleeve are visible. The actual cylindrical shapes can be found in heterogeneous and partially interrupted courses due to the small volume (few milliliter).

The results show an overall MR visibility of the IPU to provide image-based verification and validation of the current instrument position. Concerning the integration in an iMRI workflow, further visibility tests with flex coils and single loop coils are necessary.

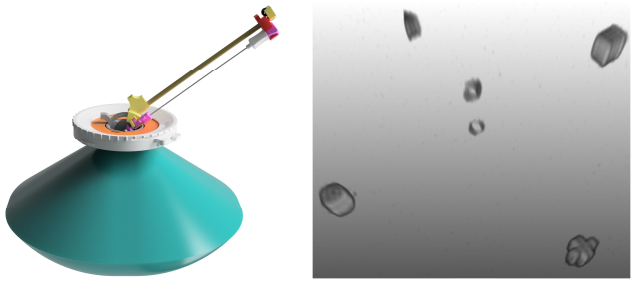

(a) (b)

Figure 5: Basic system characteristics. (a) Working volume (turquoise) with an estimated maximum needle feed of 120 mm. (b) Marker visibility in a 3D MRI data set.

3.2 Feed force

The experiment revealed that a feed force of around 14 N can be provided to ensure the potential puncture of various types of tissue, such as the heart, liver, or skin [12].

The remotely controlled DoF of the feed had been implemented for research purposes, as it is unclear how such a concept can be integrated into the workflow according to the medical device regulation requirements.

3.3 Positioning reproducibility

The position of $\varphi = 200°$ was approached from ten ($n = 10$) random rotational angles. Through the calculated spherical coordinates, the mean absolute angle deviation D_φ and the worst-case deviation e_φ were determined:

$$\boldsymbol{D_\varphi} = \frac{\mathbf{1}}{\boldsymbol{n}} \cdot \sum_{\boldsymbol{k=1}}^{\boldsymbol{n}} |\boldsymbol{\varphi_k} - \overline{\boldsymbol{\varphi}}| \quad (1)$$

$$\boldsymbol{e_\varphi} = |\boldsymbol{\varphi_{max}} - \boldsymbol{\varphi_{min}}| \quad (2)$$

The same validation sequence was applied to the analysis of the reproducibility of the angle θ, by positioning $\theta = 25°$ from randomly panned angles.

Table 1: Mean absolute deviations D_φ (rotation), D_θ (panning) and the respective worst-case deviations e_φ, e_θ.

	$\boldsymbol{\varphi}$	$\boldsymbol{\theta}$
$\boldsymbol{D}$	0.15°	0.08°
$\boldsymbol{e}$	0.5°	0.6°

The results of the mean absolute azimuth angle and polar angle deviations D_φ, D_θ from Table 1 show an angular error for repositioning of $\leq 0.15°$ on average, with rotational motion causing about twice as much deviation as panning. In the worst case, angular deviations of about $0.6°$ are to be expected.

Only the positioning in the *XY* plane was not accurately reproducible ($1-2\,\mathrm{mm}$ deviation) in this demonstrator. Possible causes are high frictional forces or jamming of the pull cords at the deflection points within the base ring. To counteract this, ceramic recirculating rings are suitable in the next demonstrator.

4 Conclusions

This work presents an MR compatible, remotely controllable µRIGS demonstrator for guiding instruments in different body regions in iMRI workflows. Thereby the compact and ultra-light IPU is designed as a patient-mounted system, which can be remotely controlled from the control room via MR safe Bowden cables and electrical stepper motors from a secure distance. Two rotational DoF and three translational DoF including the remote instrument feed are provided to cover an adequate spatial working volume. The MR visibility and positioning reproducibility tests show first results for the implementation into the iMRI environment with promising potential of instrument-micropositioning functions.

For fully automated robotic application, future research will be focused, on the one hand, on MR compatible direct positioning feedback of the mechanical components of the IPU, which provides defined and stable kinematic processes. On the other hand, registration of the IPU with the help of passive MR visible markers or alternative marker methods (e.g. resonant markers [13]) to the coordinate system of the scanner is necessary. Both parameters should serve as a component for the planning software, which performs a calculated close loop positioning of the DoFs using the planned data. Integration into an anticipated workflow will include extensive phantom testing and user studies for meaningful validation of the system's performance. Through µRIGS, the interventionist is expected to be significantly relieved both mentally and physically. In addition, robotic applications in iMRI will be demonstrated that can be integrated into the clinical workflow realistically. This increases not only efficiency, but also enables more precise punctures of e.g. small cancer foci. Risks for the patient can be minimized and the accessibility and application rate of robotic assistance systems in iMRI can be increased.

Author Statement

Research funding: The work of this paper is partly funded by the Ministry of Economics, Science and Digitization of Saxony-Anhalt under grant number l 117 and by the Federal Ministry of Education and Research within the Research Campus *STIMULATE* under the number '13GW0473A' and under the number '13GW0473B'.
Conflict of interest: Authors state no conflict of interest.

References

[1] J. Barkhausen, T. Kahn, G. A. Krombach, et al., "White paper: Interventionelle MRT: Status Quo und Entwicklungspotenzial unter ökonomischen Perspektiven, Teil 1: Generelle Anwendungen", RoFo: Fortschritte auf dem Gebiete der Röntgenstrahlen und der Nuklearmedizin, vol. 189, no. 7, pp. 611–623, 2017.

[2] U. Kägebein, O. Speck, F. Wacker, et al., "Motion correction in proton resonance frequency-based thermometry in the liver", Topics in magnetic resonance imaging: TMRI, vol. 27, no. 1, pp. 53–61, 2018.

[3] R. B. Sequeiros, R. Ojala, J. Kariniemi, et al., "MR guided interventional procedures: A review", Acta radiologica (Stockholm, Sweden: 1987), vol. 46, no. 6, pp. 576–586, 2005.

[4] R. Hoffmann, C. Thomas, H. Rempp, et al., "Performing mr-guided biopsies in clinical routine: Factors that influence accuracy and procedure time", European radiology, vol. 22, no. 3, pp. 663–671, 2012.

[5] R. Monfaredi, K. Cleary, and K. Sharma, "MRI robots for needle based interventions: Systems and technology," Annals of biomedical engineering, vol. 46, no. 10, pp. 1479–1497, 2018.

[6] N. Hata, P. Moreira, and G. Fischer, "Robotics in MRI guided interventions", Topics in magnetic resonance imaging: TMRI, vol. 27, no. 1, pp. 19–23, 2018.

[7] J. G. R. Bomers, D. G. H. Bosboom, G. H. Tigelaar, et al., "Feasibility of a 2nd generation MR-compatible manipulator for transrectal prostate biopsy guidance", European radiology, vol. 27, no. 4, pp. 1776–1782, 2017.

[8] Melzer, B. Gutmann, T. Remmele, et al., "Innomotion for percutaneous image-guided interventions: Principles and evaluation of this MR- and CT-compatible robotic system", IEEE engineering in medicine and biology magazine: the quarterly magazine of the Engineering in Medicine & Biology Society, vol. 27, no. 3, pp. 66–73, 2008.

[9] H. Mattern, R. Odenbach, P. Parsanejad, et al., "3D-printed MRI marker for personalized interventional applications through T1 and T2 relaxation time matching", International journal of computer assisted radiology and surgery proceedings, vol. 13, no. 1, pp. 171–173, 2009.

[10] R. Gassert, A. Yamamoto, D. Chapuis, et al., "Actuation methods for applications in MR environments", Concepts in Magnetic Resonance Part B: Magnetic Resonance Engineering, vol. 29B, no. 4, pp. 191–209, 2006.

[11] S. Grosu, C. Rodriguez–Guerrero, V. Grosu, et al., "Evaluation and analysis of push-pull cable actuation system used for powered orthoses", Frontiers in Robotics and AI, vol. 5, 2018.

[12] X. Bao, W. Li, M. Lu, et al., "Experiment study on puncture force between MIS suture needle and soft tissue", Biosurface and Biotribology, vol. 2, no. 2, pp. 49–58, 2016.

[13] M. Kaiser, M. Detert, M. A. Rube, et al., "Resonant marker design and fabrication techniques for device visualization during interventional magnetic resonance imaging", Biomedizinische Technik/Biomedical engineering, vol. 60, no. 2, pp. 89–103, 2015.